Interatomic potentials for rare-earth metals

1999 J. Phys.: Condens. Matter 11 6543

(http://iopscience.iop.org/0953-8984/11/34/306)

J. Phys.: Condens. Matter **11** (1999) 6543–6551. Printed in the UK PII: S0953-8984(99)05135-8

Interatomic potentials for rare-earth metals

Kan Hachiya† and Yasuhiko Ito

Department of Fundamental Energy Science, Kyoto University, Kyoto 606-8501, Japan

Received 14 June 1999

Abstract. We present semi-empirical interatomic potentials for the rare-earth metals (Sc, Y, La and lanthanides) and their compounds within the framework of the hybridized nearly-free-electron–tight-binding-bond (NFE–TBB) model. Potential parameters are adjusted to reproduce the experimental data for interatomic spacings and elastic constants. The derived potentials are found to provide good agreement with the experimental data for the face-centred cubic, hexagonal close-packed and double-hexagonal close-packed elemental rare-earth metals. We have also made a comparison between the bond-angle-dependent tight-binding-d-bond model and the bond-angle-independent model. Within the present model, we have found that the bondings in the rare-earth metals depend on the bond angles, and the dependence is weaker compared with those in the transition metals.

1. Introduction

For a few decades, bondings in simple metals have been successfully treated theoretically [1]. Harrison [2] applied one of the most simplified theories (Thomas–Fermi theory) for the simple metals and extended it to the bondings in lanthanides and heavy actinides, and succeeded in predicting the trends in some properties of these metals. His model treats the spd electrons for all the f-shell metals as the sp electrons for the simple metals, and all f bands are localized except for light actinides. In this treatment, the interatomic interaction can be written as a single-term pairwise screened Coulomb potential—the same as the one for the simple metals given by Harrison and Wills [3].

On the basis of the success of this model, Singh and Singh [4] applied the hybridized nearly-free-electron–tight-binding-bond (NFE–TBB) model of the two-body interaction to some of the fcc rare-earth metals in the form originally developed by Wills and Harrison [2, 5] and attempted to obtain a more realistic description of the bondings by treating the effect of the d bands and f bands explicitly. Using this model, they calculated the elastic constants and performed a comparison with the experimental data which showed reasonable accord.

Nevertheless, f bands for the lanthanides and heavy actinides can be seen as localized to a large extent [6] and it is questionable to treat the effect of the f bands explicitly at this level of the approximation. Besides, although the model given by Singh and Singh [4] has acquired some accuracy, no optimization of the tight-binding parameters is done and the accord with the experimental data seems to be achieved through including many-nearest-neighbour interactions. Requiring many nearest neighbours leads to the following problems, at least: (1) it is not always physical to include further-neighbour interactions instead of the angle dependence

† Present address: Department of Fundamental Energy Science, Kyoto University, Uji, Kyoto 611-0011, Japan.

0953-8984/99/346543+09$30.00

of the bondings [8], and (2) it is hard to use them as interatomic potential functions in molecular dynamics simulations.

Motivated by these facts, we have attempted to apply a simplified but realistic enough and physically appropriate interatomic potential function for rare-earth metals and their compounds. We use the formula derived using the combined NFE and bond-angle-dependent TBB model. This model was originally designed for the transition metals and their compounds, but it can be more widely used where the d or f band plays a similar role to those of the transition metals, as we have already tested for aluminium [9] and light-actinide metals [10]. The purpose of the present study is:

(1) to show how we can extend this model to the rare-earth metals with the simplification of neglecting the f-band contribution and with the emphasis on the bond-angle dependence of the d bonding by introducing angle dependence and by including only first-nearest-neighbour interactions; and
(2) to present an efficient model for, e.g., long-timescale dynamical properties, and large-scale atomistic motions, which are important for the understanding of the mechanical properties through molecular dynamics simulation using such a potential function.

In the present study, these aims are achieved through the inclusion of the long-ranged interaction in pairwise potential form and the inclusion of the short-ranged but strongly structure-dependent interaction in non-pairwise many-atom form. The latter only involves a number of atoms of the order of the coordination number.

We describe the model and the procedure that we have used for the estimations of the elastic constants to be compared with the experimental data in the next section. The results for the derived elastic constants and the comparison with the available experimental data are presented in section 3. Finally, we conclude in section 4.

2. Computational method

The hybridized NFE–TBB model of the interatomic potential is as follows [11]:

$$\Phi_{\text{total}} = \Phi_{\text{NFE}} + \Phi_{\text{TB,rep}} + \Phi_{\text{TB,bond}}. \tag{1}$$

The first term treats the sp-electron gas in simple metal. The remaining terms are for the TBB part of the potential for the d electrons in the present study, for we have assumed f bands to be fully localized. This is a good approximation except for the low-temperature phase of Ce [6]. Thus, the interatomic potential model that we have used for the rare-earth metals is the same as the one for the transition metals.

We adopt the following NFE interaction formulation given by Pettifor and Ward [12]:

$$\Phi_{\text{NFE}} = \frac{2N_{\text{s}}^2}{r_{ij}} \sum_{n=1}^{3} A_n \cos(k_n r + \alpha_n) \exp(\kappa_n r_{ij}). \tag{2}$$

N_{s} is the number of sp valence electrons. The Heine–Abarenkov model potential is used to calculate the parameters A_n, α_n, k_n and κ_n [13] and all of them are determined by r_{c} and D.

The following is the repulsive interaction used:

$$\Phi_{\text{TB,rep}} = \frac{N_{\text{d}}}{7} \frac{h_{ij}^2 d_{ij}^{10}}{r_{ij}^8}. \tag{3}$$

N_{d} is the number of d valence electrons and is determined as the number of total valence electrons minus N_{s}. d_{ij} is the equilibrium interatomic separation. We use the interatomic

matrix element form obtained by Wills and Harrison [5], and then all matrix elements and their average h are determined by a single parameter, r_{d}.

The bond energy expression is

$$\Phi_{\mathrm{TB,bond}} = 2\sum_{\alpha\beta} H_{j\beta,i\alpha}\Theta_{i\alpha,j\beta}. \tag{4}$$

$H_{j\beta,i\alpha}$ is the tight-binding Hamiltonian and $\Theta_{i\alpha,j\beta}$ is the bond order. The bond order is calculated from the following simplified expression [15]:

$$\Theta^{\alpha}_{i,j} = \widehat{\chi}(N_{\mathrm{d}}) \Bigg/ \left\{1 + \frac{1}{2}\sum_{k\neq i,j}\left[\left(\frac{h_\alpha(r_{ik})}{h_\alpha(r_{ij})}\right)^2 g_\alpha(\theta_{jik}) + \left(\frac{h_\alpha(r_{jk})}{h_\alpha(r_{ij})}\right)^2 g_\alpha(\theta_{ijk})\right]\right\}^{1/2}. \tag{5}$$

The suffix α denotes σ-, π- and δ-orbitals, and h_α corresponds to the interatomic element linking the α-orbital at each atom. $\widehat{\chi}(N_{\mathrm{d}})$ is the reduced susceptibility. $g(\theta)$ is an angle-dependent embedding function for each type of the bond. The form for g as a function of bond angle θ and the procedure for the calculation of the coefficients are given in the reference by Pettifor [14] and the resulting embedding function curves for d are presented in the literature by Nishitani *et al* [15].

We assumed that the TBB interactions are negligible except for the first-nearest neighbour and the total interactions include the contributions up to fourth-nearest neighbours as is done for the fcc structure of Al [9].

The hybridized NFE–TBB potential used in the present study is determined by three adjustable parameters, r_{c}, D and r_{d}, if we fix N_{s} or N_{d}. We set these parameters such that the interatomic spacing d and the bulk modulus B are reproduced by the least-squares fitting. We set several starting values for these parameters for each atom around the final values reported in the literature [4] and chose one which gives the best accord with experimental elastic constant data. The total number of valence electrons is 3 for all metals except Yb, for which it is 2. The value of N_{d} is 1 except for γ-Ce and β-Yb, for which it is 0.5 and 0.1 respectively. The value $N_{\mathrm{d}} = 1$ for these two metals gives very poor results for C'.

If we fix all variables r and θ in equation (5) to the interatomic separations and the bond angles of the non-strained crystallographic structure respectively, the potential function ϕ results in a pairwise interaction. We used this pairwise interaction potential for the parameter fitting, as we assumed the interatomic separations and the bulk moduli to be the same for the non-pairwise and the pairwise potential. This is true for the cubic crystals and approximately true for the hexagonal crystals. The error that arises from this assumption for the hexagonal crystals is less than 1% for all hexagonal metals; this is evaluated using the homogeneous strain matrix [7] and the equation corresponding to equation (6), as we will see later on.

The elastic constants are derived as follows. We assume that the second derivative of the binding energy per atom U for a certain deformation of the lattice structure is written as the sum of the second derivatives of the interatomic potential. Then, for cubic crystals, $C' = (1/2)(C_{11} - C_{12})$ and C_{44}, which are given by the second derivative of the binding energy with appropriate deformations, can be evaluated from the interatomic potentials. These constants are given by the following relations:

$$C_\lambda = \frac{1}{12\Omega}\frac{\mathrm{d}^2U(\gamma_\lambda)}{\mathrm{d}\gamma_\lambda^2} \qquad (\lambda = 1, 2) \tag{6}$$

where C_λ ($\lambda = 1, 2$) correspond to C' and C_{44}, and Ω is the atomic volume. The deformations γ_λ are taken as the strain matrix elements introduced in the literature [8]. The bulk moduli B are derived from

$$B = \frac{1}{12\pi d}\left(\frac{\mathrm{d}^2U}{\mathrm{d}r^2}\right)_{r=d} \tag{7}$$

where d is the equilibrium interatomic spacing.

For hexagonal crystals, elastic constants can be evaluated using the strain matrices introduced by Cohen, Stixrude and Wasserman [16], for example. We used their matrices for C_{66}, C_{44} and C_S, but we determined C_{33} instead of R using the following strain matrix:

$$\epsilon = \begin{pmatrix} 0 & 0 & 0 \\ 0 & 0 & 0 \\ 0 & 0 & \gamma \end{pmatrix} \tag{8}$$

which gives C_{33} as

$$C_{33} = \frac{1}{\Omega}\frac{\mathrm{d}^2U(\gamma)}{\mathrm{d}\gamma^2}. \tag{9}$$

The bulk moduli B for hexagonal crystals are derived in the same way as for cubic crystals. C_{11}, C_{12} and C_{13} are calculated from the following relations:

$$C_{11} = \frac{1}{2}C_S + C_{33} - \sqrt{2C_S(C_{33} - B)} + C_{66} \tag{10}$$

$$C_{12} = \frac{1}{2}C_S + C_{33} - \sqrt{2C_S(C_{33} - B)} - C_{66} \tag{11}$$

$$C_{13} = C_{33} - \sqrt{\frac{1}{2}C_S(C_{33} - B)}. \tag{12}$$

3. Results

We have chosen room temperature phases of the rare-earth metals (Sc, Y, Ce, Pr, Nd, Gd, Tb, Dy, Ho, Er, Yb, Lu) and the high-temperature cubic phase of La (fcc La) for fitting parameters for the interatomic potentials because of the best availability of experimental elastic constant data that we know of.

The final values for the parameters for each metal are compiled in table 1 and the interatomic potentials calculated using the final parameters set for β-La are presented in figure 1. The potential curve shown in figure 1 is derived with the bond orders for the

Table 1. Numbers of valence electrons used in the present calculations and the final values of the interatomic potential parameters, r_c (Å), D and r_d (Å), for the rare-earth metals derived by fitting to the experimental data for the elastic constants. Also shown are the crystal structures for each phase. The elements given without any phase specifications are room temperature phases.

	N	N_s	N_d	r_c	D	r_d	Structure
Sc	3	2	1	0.9009	0.1989	0.9898	hcp
Y	3	2	1	0.9145	0.0289	0.5132	hcp
β-La	3	2	1	1.1679	0.5826	0.8830	fcc
γ-Ce	3	2.5	0.5	1.1689	0.7861	0.8389	fcc
Pr	3	2	1	1.0210	0.3776	0.6283	dhcp
Nd	3	2	1	1.0225	0.3540	0.7406	dhcp
Gd	3	2	1	0.9666	0.1688	0.7955	hcp
Tb	3	2	1	0.9397	0.1656	0.6906	hcp
Dy	3	2	1	0.9266	0.1209	0.7005	hcp
Ho	3	2	1	0.9016	0.0843	0.5869	hcp
Er	3	2	1	0.9029	0.0536	0.7186	hcp
β-Yb	2	1.9	0.1	1.2036	0.6764	0.7291	fcc
Lu	3	2	1	0.9170	0.1989	0.8397	hcp

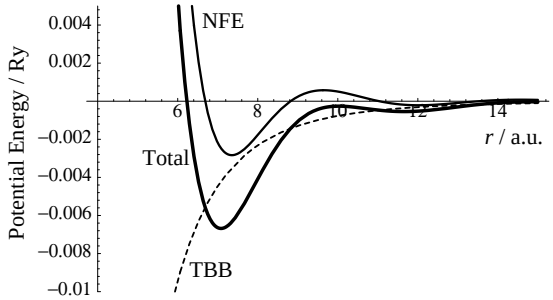

Figure 1. The interatomic potential for β-La calculated with the final set of parameters.

bonding with the first-nearest-neighbour atoms. Consequently, the same curve shows the angle-dependent non-pairwise potential describing the first-nearest-neighbour bond axis direction and the angle-independent pairwise potential for all directions at the same time.

The change of the binding energy versus the tetragonal or trigonal shear strain calculated with the non-pairwise interaction potential model for β-La is given in figure 2. The second-order polynomial fit shown in the figure is obtained by a least-squares fitting to the plotted binding energy change.

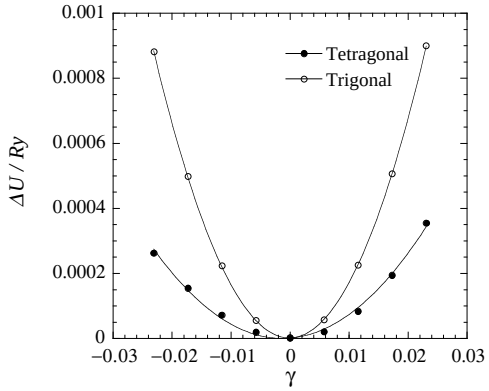

Figure 2. Change of the binding energy per atom as a function of γ for tetragonally and trigonally deformed β-La. The curves given are second-order polynomial fits.

The elastic constants calculated using these binding energy curves are given in tables 2 and 3 with the experimental data. The calculated and experimental elastic constant data show good agreement for all the rare-earth metals as a whole, as we show in figure 3, but the data for C_{44} do not show good accord like the other constants. Our choice of the model and the parameters almost always results in too-low calculated values. The non-pairwise and the pairwise potentials show some difference in agreement between the calculated and the experimental data for tetragonal shear constants C' for cubic metals or C_{66} for hexagonal metals. The difference is also shown in C_{44}. The non-pairwise potentials give lower values of C_{44} compared with those with the pairwise potentials. This means that the effect of the non-pairwise interactions does exist, but it is more complicated than we have assumed. There may be higher moments to be included in the evaluation of the bond orders of the bondings in these metals.

Table 2. Calculated and experimentally determined elastic constants C_{ij} (GPa), the result of the fitting and the experimental data for the interatomic separations d (au) and the bulk moduli B (GPa) for the cubic crystals. The experimental data for d are calculated from the experimental lattice constant [17]. Calculated also are the elastic constants obtained from the pairwise potentials with fixed bond order. 'n' and 'p' stand for the non-pairwise and the pairwise potential respectively. The parameters used are those compiled in table 1 and the same for the present two models.

		C_{11}	C_{12}	C_{44}	B	C'	d
β-La	n	30.66	19.32	16.37	23.10	5.67	7.0705
	p	32.57	18.37	18.22	23.10	7.10	7.0705
	Experiment[a]	28.46	20.41	16.53	23.09	4.03	7.0707
γ-Ce	n	26.87	13.67	12.08	18.07	6.60	6.8913
	p	27.96	13.13	13.14	18.07	7.42	6.8913
	Experiment[b]	26.01	14.26	17.30	18.18	5.88	6.8891
β-Yb	n	18.59	10.26	10.04	13.04	4.17	7.3297
	p	18.73	10.19	10.18	13.04	4.27	7.3297
	Experiment[c]	18.62	10.36	17.72	13.11	4.13	7.3270

[a] Elastic constant data from [18] (660 K).
[b] Elastic constant data from [19].
[c] Elastic constant data from [20].

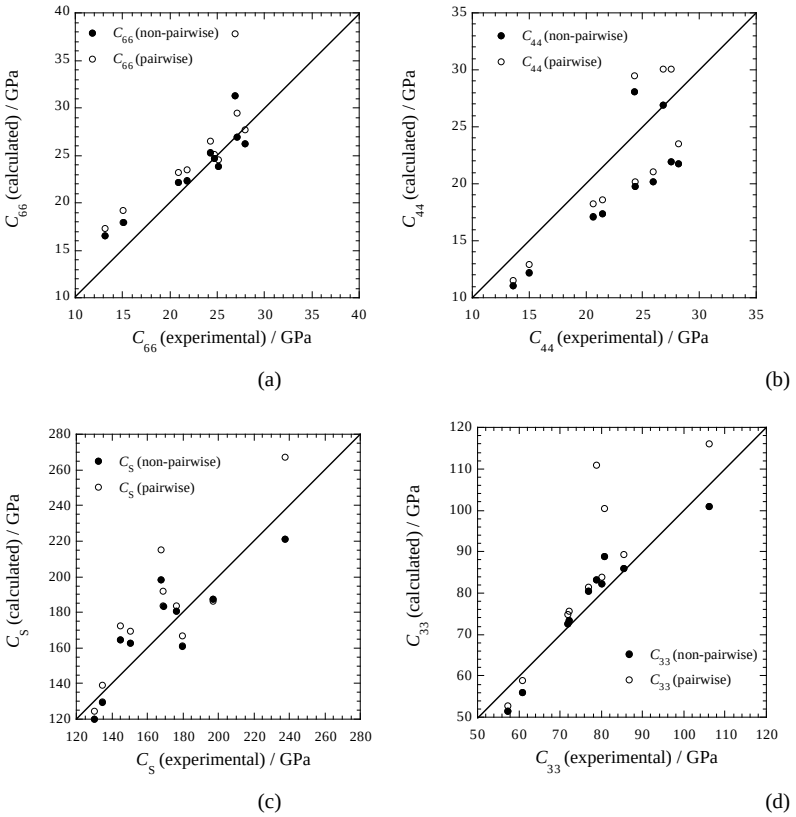

Figure 3. Plots of the experimental versus calculated elastic constants for (a) C_{66}, (b) C_{44}, (c) C_S and (d) C_{33}.

Table 3. Calculated and experimentally determined elastic constants C_{ij} (GPa), the result of the fitting and the experimental data for the interatomic separations d (au) and the bulk moduli B (GPa) for the hexagonal crystals. The experimental data for d and c/a are calculated from the experimental lattice constant [17]. Calculated also are the elastic constants obtained from the pairwise potentials with fixed bond order. 'n' and 'p' stand for the non-pairwise and the pairwise potential respectively. The parameters used are those compiled in table 1 and the same for the present two models.

		C_{11}	C_{12}	C_{13}	C_{33}	C_{44}	B	C_{66}	d	c/a
Sc	n	103.0	40.4	31.0	100.9	21.9	56.72	31.3	6.251	1.584
	p	109.4	33.8	27.0	116.1	30.1	56.72	37.8	6.251	1.584
	Experiment[a]	98.6	44.8	29.5	106.2	27.5	56.72	26.9	6.251	1.592
Y	n	76.60	27.41	21.09	80.59	19.71	41.43	24.59	6.90036	1.61334
	p	77.06	27.01	20.83	81.47	20.18	41.43	25.02	6.90036	1.61334
	Experiment[b]	77.90	28.50	21.00	76.90	24.31	41.43	24.70	6.90038	1.57399
Pr	n	54.19	21.18	14.58	51.55	11.06	28.80	16.50	6.9400	1.6275
	p	55.10	20.59	14.09	52.72	11.46	28.80	17.26	6.9400	1.6275
	Experiment[c]	49.35	22.95	14.3	57.40	13.60	28.80	13.20	6.9400	1.6114
Nd	n	59.47	23.63	16.40	56.02	12.17	31.78	17.92	6.9131	1.6264
	p	60.88	22.52	15.41	58.83	12.94	31.78	19.18	6.9131	1.6264
	Experiment[d]	54.82	24.62	16.6	60.86	15.03	31.79	15.10	6.9130	1.6124
Gd	n	69.73	25.44	19.41	72.62	17.11	37.83	22.15	6.8654	1.6179
	p	70.86	24.48	18.78	74.73	18.26	37.83	23.19	6.8654	1.6179
	Experiment[b]	66.67	24.99	21.32	71.91	20.69	37.83	20.84	6.8654	1.5893
Tb	n	71.25	26.55	19.97	73.28	17.34	38.72	22.35	6.80496	1.61906
	p	72.51	25.47	19.26	75.62	18.63	38.72	23.52	6.80496	1.61906
	Experiment[e]	67.88	24.32	22.99	72.25	21.40	38.78	21.78	6.80496	1.58111
Dy	n	75.94	25.39	21.01	83.08	28.09	41.07	25.28	6.7896	1.5842
	p	69.63	16.64	29.08	110.97	29.49	41.07	26.49	6.7896	1.5842
	Experiment[b]	74.66	26.16	22.33	78.71	24.27	41.07	24.25	6.7896	1.5732
Ho	n	71.16	23.48	24.41	82.08	20.15	40.81	23.84	6.7601	1.5808
	p	71.93	22.76	24.02	83.89	21.09	40.81	24.58	6.7601	1.5808
	Experiment[f]	76.12	26.00	20.72	80.15	25.92	40.81	25.06	6.7601	1.5698
Er	n	82.70	30.22	24.38	85.99	21.73	45.47	26.24	6.7252	1.5810
	p	82.35	27.02	25.38	89.31	23.51	45.47	27.66	6.7252	1.5810
	Experiment[b]	86.34	30.50	22.70	85.54	28.09	45.47	27.92	6.7252	1.5700
Lu	n	87.00	33.05	24.94	88.87	26.97	47.59	26.97	6.6326	1.5860
	p	86.72	27.77	25.24	100.36	30.11	47.59	29.48	6.6326	1.5860
	Experiment[g]	86.23	32.03	28.0	80.86	26.79	47.59	27.10	6.6326	1.5860

[a] Elastic constant data from [21] (303 K).
[b] Elastic constant data from [22] (298.0 K).
[c] Elastic constant data from [23] (300 K).
[a] Elastic constant data from [24] (300 K).
[b] Elastic constant data from [25] (300 K).
[c] Elastic constant data from [26] (300 K).
[c] Elastic constant data from [27] (300.1 K).

Although the effect of the angle dependence of the d bond is revealed, it is not so evident as for the transition metals or the light-actinide metals, for example. The relatively weak dependence on the angle-dependent d bond in the rare-earth metals corresponds to the small values of r_{d} in table 1 compared with those of the transition metals [11]. This means that

the contributions of the d bands in the rare-earth metals are smaller compared with those in the transition metals. Therefore, the d bonding in the rare-earth metals can be said to play a non-negligible role in the sense that it adds the angular character to the total bonding, but it is a relatively small role at the same time.

For practical use as a potential function in molecular dynamics simulations, the pairwise model may be used instead of the non-pairwise model, as the calculated data show better accord with experimental data compared with the case of the transition metals, because of the relatively small contribution of the d bonding. In addition, one may be able to adopt shorter cut-off radii of the potentials. As we have shown for light-actinide metals [10] and Al [9], we can easily fit to the equilibrium interatomic separations, and the elastic constants (i.e. the second derivative of the potential) are insensitive to the number of nearest neighbours included. Therefore, we can expect that the force acting near the equilibrium atomic positions, at least, can be calculated exactly enough.

4. Conclusions

We have presented the hybridized NFE–TBB potentials for the rare-earth metals and their compounds and tested them through comparison between calculated and experimental elastic constant data.

We can successfully fit to or reproduce the experimental data for the equilibrium interatomic separations, bulk moduli and elastic constants for the cubic and the hexagonal crystals, and the c/a ratio for the hexagonal crystals.

The bondings in the rare-earth metals are proved to depend on the angle dependence of the d bond, and they are obscure compared with those in the transition metals at the same time.

The interatomic interaction model used in the present study is based on the angle-dependent second-moment approximation of the bond order, but higher orders of the moment may be needed especially for the prediction of C_{44} for cubic crystals, which have highly negative Cauchy pressures ($C_{12} - C_{44}$), such as γ-Ce or β-Yb.

The model presented and tested in the present study is easily extended to the rare-earth compounds, as has been demonstrated for the transition metals [11, 28].

Acknowledgments

Some of the computations in the present study were done at the Kyoto University Data Processing Centre. We have also used *Mathematica* for Solaris running on the SUN Ultra Enterprise 3000 at the Supercomputer Laboratory, Institute for Chemical Research, Kyoto University for some of the computations.

References

[1] Harrison W A 1980 *Electronic Structure and the Properties of Solids* (New York: Freeman)
[2] Harrison W A 1983 *Phys. Rev.* B **28** 550
[3] Harrison W A and Wills J M 1982 *Phys. Rev.* B **25** 5007
[4] Singh N and Singh S P 1990 *Phys. Rev.* B **42** 1652
[5] Wills J M and Harrison W A 1983 *Phys. Rev.* B **28** 4363
[6] Harrison W A 1984 *Phys. Rev.* B **29** 2917
[7] Hasegawa H, Finnis M W and Pettifor D G 1985 *J. Phys. F: Met. Phys.* **15** 19
[8] Alinaghian P, Nishitani S R and Pettifor D G 1994 *Phil. Mag.* B **69** 889
[9] Hachiya K and Ito Y 1999 unpublished
[10] Hachiya K and Ito Y 1999 *Physica* B **262** 233

[11] Hausleitner Ch and Hafner J 1992 *Phys. Rev.* B **45** 115
[12] Pettifor D G and Ward M A 1984 *Solid State Commun.* **49** 291
[13] Singh N, Banger N S and Singh S P 1989 *Phys. Rev.* B **39** 3097
[14] Pettifor D G 1990 *Many-Atom Interactions in Solids* ed R M Nieminen, M J Puska and M J Manninen (Berlin: Springer) p 64
[15] Nishitani S R, Alinaghian P, Hausleitner C and Pettifor D G 1994 *Phil. Mag. Lett.* **69** 177
[16] Cohen R E, Stixrude L and Wasserman E 1997 *Phys. Rev.* B **56** 8575
[17] Villars P and Calvert L D 1991 *Pearson's Handbook of Crystallographic Data for Intermetallic Phases* 2nd edn (Materials Park, OH: ASM International)
[18] Stassis C, Loong C-K and Zarestky J 1982 *Phys. Rev.* B **26** 5426
[19] Greiner J D, McMasters O D and Smith J F 1980 *Scr. Metall.* **14** 989
[20] Stassis C, Loong C-K, Theisen C and Nicklow R M 1982 *Phys. Rev.* B **26** 4106
[21] Leisure R G, Schwarz R B, Migliori A and Lei M 1993 *Phys. Rev.* B **48** 1276
[22] Simmons G and Wang H 1971 *Single Crystal Elastic Constants and Calculated Aggregate Properties: a Handbook* (Cambridge, MA: MIT Press)
[23] Greiner J D, Schiltz R J Jr, Tonnies J J, Spedding F H and Smith J F 1973 *J. Appl. Phys.* **44** 3862
[24] Greiner J D, Schlader D M, McMasters O D, Gschneidner K A Jr and Smith J F 1976 *J. Appl. Phys.* **47** 3427
[25] Salama K, Brotzen F R and Donoho P L 1972 *J. Appl. Phys.* **43** 3254
[26] Salama K, Brotzen F R and Donoho P L 1973 *J. Appl. Phys.* **44** 180
[27] Tonnies J J, Gschneidner K A Jr and Spedding F H 1971 *J. Appl. Phys.* **42** 3275
[28] Hachiya K and Ito Y 1998 *J. Alloys Compounds* **279** 171